

# Experiences with a space-time multigrid method for the optimal control of a chemical turbulence model

A. Borzi<sup>1,\*</sup> and R. Griesse<sup>2</sup>

<sup>1</sup> *Institut für Mathematik und Wissenschaftliches Rechnen, Karl-Franzens-Universität Graz, Heinrichstr. 36, 8010 Graz, Austria*

<sup>2</sup> *Johann Radon Institute for Computational and Applied Mathematics (RICAM), Austrian Academy of Sciences, Altenbergerstr. 69, 4040 Linz, Austria*

## SUMMARY

Lambda-omega systems provide a universal model to investigate two-species reaction diffusion problems. In the case of fast reaction kinetics and small diffusion, these systems evolve to turbulent behavior. A class of open-loop optimal control problems governed by lambda-omega systems in the turbulent regime is investigated. Optimal solutions are characterized by optimality systems consisting of two pairs of reaction diffusion equations with opposite time orientation. These systems are solved by a space-time multigrid scheme suitable for the turbulent setting. Numerical examples are given where the control drives the chaotic system to form regular patterns. Copyright © 2000 John Wiley & Sons, Ltd.

KEY WORDS: Chemical turbulence; optimal control problems; multigrid methods.

## 1. INTRODUCTION

Many biological [11], chemical [8], and physiological [12] processes can be modelled by reaction diffusion systems where the reaction kinetics exhibit a periodic limit cycle behavior via a Hopf bifurcation. In the case of two-species dynamics, in the vicinity of the Hopf bifurcation, these models are similar to lambda-omega systems; see [4]. We consider lambda-omega ( $\lambda$ - $\omega$ ) systems with distributed control of the form

$$\frac{\partial}{\partial t} \begin{pmatrix} y_1 \\ y_2 \end{pmatrix} = \begin{bmatrix} \lambda(s) & -\omega(s) \\ \omega(s) & \lambda(s) \end{bmatrix} \begin{pmatrix} y_1 \\ y_2 \end{pmatrix} + \sigma \Delta \begin{pmatrix} y_1 \\ y_2 \end{pmatrix} + R \begin{pmatrix} u_1 \\ u_2 \end{pmatrix} \quad \text{in } Q = \Omega \times (0, T), \quad (1)$$

where  $s^2 = y_1^2 + y_2^2$ ,  $\lambda(s)$  and  $\omega(s)$  are real functions of  $s$ , and  $u_1, u_2 \in L^2(U)$ ,  $U = \Omega' \times (0, T)$ ,  $\Omega' \subset \Omega$ , represent distributed control functions with support on the subdomain  $\Omega'$ . Here,  $\sigma$  is the diffusion coefficient and  $R : L^2(U) \rightarrow L^2(Q)$  is an extension operator defined as follows:

---

\*Correspondence to: Alfio Borzi, Institut für Mathematik und Wissenschaftliches Rechnen, Karl-Franzens-Universität Graz, Heinrichstr. 36, 8010 Graz, Austria. E-mail: [alfio.borzi@uni-graz.at](mailto:alfio.borzi@uni-graz.at)

Contract/grant sponsor: "Optimization and Control" FWF Fund; contract/grant number: SFB F003

$Ru_i = u_i$  in  $U$  and  $Ru_i = 0$  in  $Q \setminus U$ . We focus on a representative functional form of  $\lambda$  and  $\omega$  which was proposed in [9] to model chemical turbulence:

$$\lambda(s) = 1 - s^2 \quad \text{and} \quad \omega(s) = -\beta s^2. \quad (2)$$

Equations (1)–(2) can also be written in their complex form

$$\psi_t = \psi - (1 + i\beta)|\psi|^2 \psi + \sigma \Delta \psi, \quad (3)$$

where  $\psi = y_1 + iy_2$ , which is a special case of the complex Ginzburg-Landau model. These equations have a long history in physics as a generic amplitude equation near the onset of instabilities that lead to chaotic dynamics in fluid mechanical systems; see, e.g., [10]. Taking the complex conjugate of (3) and changing the sign before  $\beta$  keeps the equation of motion invariant. Thus, only  $|\beta|$  is the essential parameter.

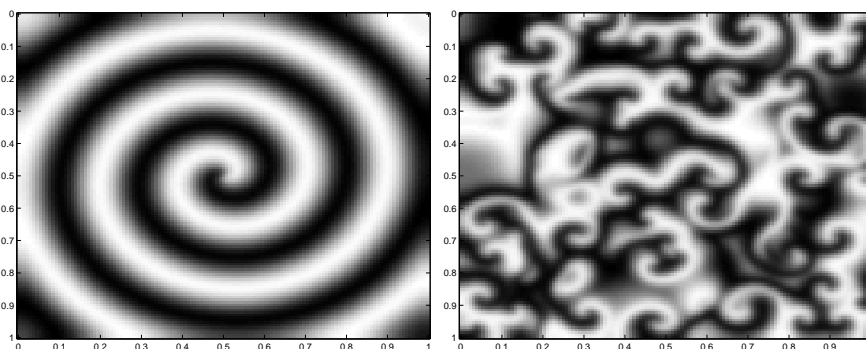


Figure 1. Solution  $y_1$  of (1)–(2) without control for  $\beta = 1$  (left) and  $\beta = 2$  (right) and  $\sigma = 10^{-4}$  with homogeneous Neumann boundary conditions, at  $t = 200$  and  $\Omega = (0, 1)^2$ . Initial conditions are given by  $y_1 = (x_1 - 1/2)/10$  and  $y_2 = (-x_2 + 1/2)/20$ . (Dark regions correspond to negative values, bright regions correspond to positive values.)

System (1)–(2) possesses spiral wave solutions which persist indefinitely. In Figure 1, snapshots of uncontrolled solutions for the case  $\beta = 1$  (left) and for  $\beta = 2$  (right) are shown.

As  $\beta$  becomes larger than a threshold value, spiral wave solutions become unstable and nucleate spontaneously as finite singularities of the evolution of the temporal phase ( $\psi = s e^{i\phi(t)}$ ) giving rise to turbulence; see Figure 1 (right). The occurrence of spatio-temporal structures, like plane waves, spiral waves, and sustained turbulence, is due to instability inherent to the system. In order to obtain solutions whose amplitudes persist indefinitely the diffusion rate  $\sigma$  has to be chosen sufficiently small. While this condition is necessary to have pattern-like solutions, the onset of chemical turbulence is due to instability of these solutions as  $\beta$  becomes sufficiently large.

We discuss open-loop control problems governed by lambda-omega systems in the turbulent regime. In the context of chemical reactions involving ionic species, the control may represent an electric field. In this case, control may be required to drive the system to form a desired pattern, or to avoid transition to chaos, which would destroy desired electrical properties [6].

To formulate the optimal control problem, we define the following objective function

$$J(y, u) = \sum_{i=1}^2 \left( \frac{1}{2} \|y_i - y_{id}\|_{L^2(Q)}^2 + \frac{\gamma_i}{2} \|Ru_i\|_{L^2(Q)}^2 \right), \quad (4)$$

where  $y = (y_1, y_2)$  and  $u = (u_1, u_2)$ , and  $y_{id} \in L^2(Q)$  represent desired trajectories. The values of the weights  $\gamma_i > 0$  determine the ‘importance’ of the cost of the controls.

Our optimal control problem is formulated as follows

$$\begin{cases} \min_{u \in [L^2(U)]^2} J(y, u), \\ \text{under the constraint that the } \lambda - \omega \text{ system (1)–(2) is satisfied.} \end{cases} \quad (5)$$

Solutions to (5) are characterized by optimality systems, representing first order necessary conditions for a minimum. In the present case, the optimality system consists of (1)–(2), the following adjoint equations for the adjoint variables  $p = (p_1, p_2)$  (marching backwards)

$$\begin{aligned} -\frac{\partial}{\partial t} \begin{pmatrix} p_1 \\ p_2 \end{pmatrix} &= \begin{bmatrix} 1 - 3y_1^2 - y_2^2 + 2\beta y_1 y_2 & -3\beta y_1^2 - \beta y_2^2 - 2y_1 y_2 \\ \beta y_1^2 + 3\beta y_2^2 - 2y_1 y_2 & 1 - y_1^2 - 3y_2^2 - 2\beta y_1 y_2 \end{bmatrix} \begin{pmatrix} p_1 \\ p_2 \end{pmatrix} \\ &+ \sigma \Delta \begin{pmatrix} p_1 \\ p_2 \end{pmatrix} - \begin{pmatrix} y_1 - y_{1d} \\ y_2 - y_{2d} \end{pmatrix} \quad \text{in } Q, \end{aligned} \quad (6)$$

and the optimality conditions

$$\gamma_1 u_1 - R^* p_1 = 0 \quad \text{and} \quad \gamma_2 u_2 - R^* p_2 = 0, \quad (7)$$

where  $R^*$  denotes the adjoint of  $R$  (the restriction from  $Q$  to  $U$ ); for the derivation of (6) and (7) see [2]. On the lateral boundary of  $Q$ , homogeneous Neumann boundary conditions are imposed for  $y$  and thus for  $p$ . In addition,  $y_0 = (y_{10}, y_{20})$  denotes the initial conditions for the state variables and the terminal condition for the adjoint variables is given by  $(p_1(\cdot, T), p_2(\cdot, T)) = (0, 0)$  in  $\Omega$ . In the sequel, we refer to (1)–(2), (6), and the optimality conditions (7), including the initial, terminal, and boundary conditions, as the optimality system.

## 2. DISCRETIZATION AND MULTIGRID METHOD

The optimality system is discretized by finite differences and the Euler scheme. Let us denote by  $\{\Omega_h\}_{h>0}$  a sequence of uniform grids and assume for simplicity that  $\Omega$  is a square. The Laplacian with homogeneous Neumann boundary conditions is approximated by the common five-point stencil and denoted by  $\Delta_h$ . Neumann boundary conditions are implemented by considering the differential equations on the boundary and using second-order centered finite differences to eliminate the (ghost) variables outside of the domain.

Let us denote by  $\delta t = T/N_t$  the time step size and define the space-time grid

$$Q_{h,\delta t} = \{(\mathbf{x}, t_m) : \mathbf{x} \in \Omega_h, t_m = (m-1)\delta t, 1 \leq m \leq N_t + 1\}.$$

On this grid,  $y_h^m$  and  $p_h^m$  denote the state and adjoint grid functions at time level  $m$ . The action of the backward and forward time difference operators on  $y_h^m$  and  $p_h^m$  is defined by

$$\partial_t^+ y_h^m = \frac{y_h^m - y_h^{m-1}}{\delta t} \quad \text{and} \quad \partial_t^- p_h^m = \frac{p_h^{m+1} - p_h^m}{\delta t},$$

respectively; see [1] for more details. For grid functions defined on  $Q_{h,\delta t}$  we use the discrete  $L^2(Q)$  scalar product with norm  $\|v_{h,\delta t}\|_0 = (v_{h,\delta t}, v_{h,\delta t})_{L^2_{h,\delta t}(Q_{h,\delta t})}^{1/2}$  where

$(v_{h,\delta t}, w_{h,\delta t})_{L^2_{h,\delta t}(Q_{h,\delta t})} = \delta t h^2 \sum_{(\mathbf{x},t) \in Q_{h,\delta t}} v_h(\mathbf{x},t) w_h(\mathbf{x},t)$ . In what follows, we assume for simplicity sufficient regularity of the data,  $y_{iT}, y_{id}, y_{i0}$ , such that these functions are properly approximated by their values at grid points.

The optimality system is characterized by reaction diffusion equations with opposite time orientation. Because of the presence of the reaction terms, a forward-backward sequential solution approach does not allow a robust implementation of the time coupling between the state and adjoint variables. For this reason a space-time multigrid scheme was proposed in [1] to solve parabolic optimality systems in one shot in the whole space-time domain.

The core element of the multigrid approach in [1] was a pointwise collective Gauss-Seidel smoothing applied to the set of state and adjoint variables, consistently with the opposite time-orientation. However, for small  $\sigma$  required for turbulent evolution, pointwise smoothing is not appropriate because the coupling in the space directions is too weak. To overcome this problem, collective  $t$ -line-relaxation of the optimal control variables is considered. One step of this smoothing procedure, denoted by  $S$ , can be described as follows. At the space grid-point indexed by  $ij$ , consider the discrete optimality system for all time steps. For simplicity, we can plug in the optimality conditions (7) into (1) to eliminate the control variables. Therefore we obtain a block-tridiagonal system at each spatial grid point  $ij$ , where each block is a  $4 \times 4$  matrix corresponding to the two pairs  $(y_1, y_2)$  and  $(p_1, p_2)$  at a certain time level. Notice that we consider the terms within brackets  $[\ ]$  in (1) and (6) as frozen during the smoothing step. Block-tridiagonal systems can be solved efficiently with  $\mathcal{O}(N_t)$  effort.

We now give a short description of our algorithm based on the full approximation storage (FAS) multigrid framework [3]. Let us consider  $L$  grid levels indexed by  $k = 1, \dots, L$ , where  $k = L$  refers to the finest grid. The mesh of level  $k$  is denoted by  $Q_k = Q_{h_k, \delta t_k}$  where  $h_k = h_1/2^{k-1}$  and  $\delta t_k = \delta t$ , thus we employ semicoarsening in space. Any operator and variable defined on  $Q_k$  is indexed by  $k$ .

The optimality system at level  $k$  with given initial, terminal, and boundary conditions is represented by the following nonlinear equation

$$A_k(w_k) = f_k, \quad w_k = (y_k, p_k). \quad (8)$$

The action of one FAS-cycle applied to (8) is expressed in terms of the (nonlinear) multigrid iteration operator  $B_k$ . Starting with an initial approximation  $w_k^{(0)}$ , the result of one FAS- $V(\nu_1, \nu_2)$ -cycle is denoted by  $w_k = B_k(w_k^{(0)}) f_k$ .

#### Multigrid FAS- $V(\nu_1, \nu_2)$ -Cycle

Set  $B_1(w_1^{(0)}) \approx A_1^{-1}$  (e.g., iterating with  $S_1$  starting with  $w_1^{(0)}$ ). For  $k = 2, \dots, L$  define  $B_k$  in terms of  $B_{k-1}$  as follows.

1. Set the starting approximation  $w_k^{(0)}$ .
2. Pre-smoothing. Define  $w_k^{(l)}$  for  $l = 1, \dots, \nu_1$ , by  $w_k^{(l)} = S_k(w_k^{(l-1)}, f_k)$ .
3. Coarse grid correction. Set  $w_k^{(\nu_1+1)} = w_k^{(\nu_1)} + I_{k-1}^k (q - \hat{I}_k^{k-1} w_k^{(\nu_1)})$  where

$$q = B_{k-1}(\hat{I}_k^{k-1} w_k^{(\nu_1)}) \left[ I_k^{k-1} (f_k - A_k(w_k^{(\nu_1)})) + A_{k-1}(\hat{I}_k^{k-1} w_k^{(\nu_1)}) \right].$$

4. Post-smoothing. Define  $w_k^{(l)}$  for  $l = \nu_1 + 2, \dots, \nu_1 + \nu_2 + 1$ , by  $w_k^{(l)} = S_k(w_k^{(l-1)}, f_k)$ .
5. Set  $B_k(w_k^{(0)}) f_k = w_k^{(\nu_1 + \nu_2 + 1)}$ .

In our implementation, we choose  $I_k^{k-1}$  to be the full-weighted restriction operator [5] in space with no averaging in the time direction. The mirrored version of this operator applies also to the boundary points. We choose  $\hat{I}_k^{k-1}$  to be straight injection. The prolongation  $I_{k-1}^k$  is defined by bilinear interpolation in space. No interpolation in time is needed. Indeed, other choices of prolongation and restriction operators are possible; see in particular [7].

### 3. NUMERICAL EXPERIMENTS

Results of experiments are reported to demonstrate some convergence properties of our algorithm and in general to evaluate the ability of the distributed control functions to drive the system from a chaotic state to an ordered one. The tracking ability is expressed in terms of values of the tracking functional,  $\|y_i - y_{id}\|_0$ .

All experiments are performed with the FAS- $V(2, 2)$ -cycle multigrid scheme described in the previous section. The coarsest space grid consists of four intervals in each direction.

The initial conditions for the state variables on  $\Omega = (0, 1) \times (0, 1)$  are defined as the solution of the freely evolving lambda-omega system with  $\beta = 2$  at  $t_0 = 200$ , starting with

$$y_1 = (x_1 - 1/2)/10 \text{ and } y_2 = (-x_2 + 1/2)/20.$$

The resulting disordered states (see Figure 1) represent the initial conditions for the optimal control problem of tracking the following desired state trajectories

$$\begin{aligned} y_{1d}(\mathbf{x}, t) &= \begin{cases} \sin^2(2\pi t) & \text{if } |x_1 - x_2| < 0.2 \text{ or } |x_1 + x_2 - 1| < 0.2 \\ 0 & \text{otherwise} \end{cases} \\ y_{2d}(\mathbf{x}, t) &= \begin{cases} 0 & \text{if } |x_1 - 0.5| < 0.1 \text{ or } |x_2 - 0.5| < 0.1 \\ \cos^2(2\pi t) & \text{otherwise.} \end{cases} \end{aligned}$$

In the first series of experiments  $\Omega' = \Omega$  and  $R$  is the identity on  $L^2(Q)$ . The optimal control problem is considered in the interval  $[t_0, t_0 + 1]$ . Results for this case are reported in Table I. We observe fast convergence independent of the mesh size, which improves as the values of  $\gamma_i$  become smaller. This fact shows robustness of the multigrid scheme with block smoothing with respect to the weights  $\gamma_i$  of the control. Further numerical experiments show that the multigrid iteration is not sensitive to the value of the reaction parameter  $\beta$  and to the mesh size. All these facts are in agreement with results of local Fourier analysis given in [1, 2]. Similarly we can show that as  $\sigma$  increases, the convergence properties of the space-time multigrid scheme approach those of standard multigrid scheme for Poisson problems. Notice in Table I that, as the values of  $\gamma$  increase, naturally larger values of the tracking errors are obtained.

Next we consider the case where the control acts on the annular domain given by

$$\Omega' = \{\mathbf{x} \in \Omega : -\cos(3\pi\sqrt{(x_1 - 1/2)^2 + (x_2 - 1/2)^2} + \pi/6) > 0\}.$$

Although the coupling between the state and the control variables is weaker now, the computational performance of the space-time multigrid remains similar as in the previous case. To show the tracking behavior we depict in Figure 2 snapshots of the controlled state  $y_1$ . We observe that on the subdomain  $\Omega'$ , the distributed control drives the system from a chaotic state to an ordered one. However, the presence of the control does not appear to affect the evolution of the turbulent patterns outside of the support of  $u$ . A similar phenomenon can

Table I. Convergence and tracking properties depending on  $\gamma_1 = \gamma_2 = \gamma$ ;  $\beta = 2$ ,  $\sigma = 10^{-4}$ . Here  $\rho$  is the average multigrid convergence factor [5].

$\gamma$	$N_x \times N_y \times N_t$	$\rho$	$\ y_1 - y_{1d}\ _0$	$\ y_2 - y_{2d}\ _0$
$10^{-1}$	$64 \times 64 \times 50$	0.04	$3.65 \cdot 10^{-1}$	$3.92 \cdot 10^{-1}$
$10^{-3}$	$64 \times 64 \times 50$	0.006	$6.26 \cdot 10^{-2}$	$1.03 \cdot 10^{-1}$
$10^{-5}$	$64 \times 64 \times 50$	$< 0.001$	$1.91 \cdot 10^{-3}$	$3.65 \cdot 10^{-3}$
$10^{-7}$	$64 \times 64 \times 50$	$< 0.001$	$2.01 \cdot 10^{-5}$	$3.84 \cdot 10^{-5}$
$10^{-1}$	$128 \times 128 \times 100$	0.15	$3.78 \cdot 10^{-1}$	$4.04 \cdot 10^{-1}$
$10^{-3}$	$128 \times 128 \times 100$	0.004	$7.28 \cdot 10^{-2}$	$1.20 \cdot 10^{-1}$
$10^{-5}$	$128 \times 128 \times 100$	$< 0.001$	$4.84 \cdot 10^{-3}$	$8.85 \cdot 10^{-3}$
$10^{-7}$	$128 \times 128 \times 100$	$< 0.001$	$5.74 \cdot 10^{-5}$	$1.05 \cdot 10^{-4}$

be experienced in the case of boundary control which thus seems unsuitable to influence the chaotic lambda-omega system in any meaningful way. This can be attributed to the very small diffusivity in the system.

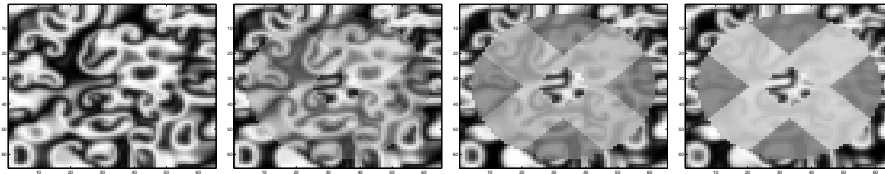


Figure 2. Controlled state  $y_1$  at  $t = 0, 0.18, 0.48, 0.78$ .

#### REFERENCES

1. Borzì A. Multigrid methods for parabolic distributed optimal control problems. *J. Comp. Appl. Math.* 2003; **157**:365–382.
2. Borzì A, Griesse R. Distributed optimal control of lambda-omega systems. Submitted to Journal of Numerical Mathematics. (<http://www.ricam.oeaw.ac.at/people/page/griesse/publications/oclosn.pdf>)
3. Brandt A. Multi-level adaptive solutions to boundary-value problems. *Mathematics of Computation* 1977; **31**:333–390.
4. Duffy A, Britton K, Murray J. Spiral wave solutions of practical reaction-diffusion systems. *SIAM J. Appl. Math.* 1980; **39**(1):8–13.
5. Hackbusch W. *Multi-Grid Methods and Applications*, Springer-Verlag, 1985.
6. Hagberg A, Meron E, Rubinstein I, Zaltzman B. Controlling domain patterns far from equilibrium. *Phys. Rev. Lett.* 1996; **76**:427–430.
7. Horton G, Vandewalle S. A space-time multigrid method for parabolic partial differential equations. *SIAM J. Sci. Comput.* 1995, **16**(4):848–864.
8. Kuramoto Y. *Chemical Oscillations, Waves, and Turbulence*, Springer-Verlag, 1984.
9. Kuramoto Y, Koga S. Turbulized rotating chemical waves. *Prog. Theor. Phys.* 1981; **66**(3):1081–1085.
10. Mielke A, Schneider G. Derivation and justification of the complex Ginzburg–Landau equation as a modulation equation. *Lectures in Applied Mathematics* 1996; **31**:191–216.
11. Murray JD. *Mathematical Biology*, Springer-Verlag, 1993.
12. Panfilov AV. Electrophysiological model of the heart and its application to studying of cardiac arrhythmias, *Workshop on Issues in Cardiovascular - Respiratory Control Modeling*, June 14–16, 2001, Graz, Austria.